

See discussions, stats, and author profiles for this publication at: <https://www.researchgate.net/publication/231392981>

Molecular Weight Control in a Starved Emulsion Polymerization of Styrene

ARTICLE *in* INDUSTRIAL & ENGINEERING CHEMISTRY RESEARCH · AUGUST 1998

Impact Factor: 2.59 · DOI: 10.1021/ie980009y

CITATIONS

35

READS

65

4 AUTHORS, INCLUDING:



Luis Gugliotta

National Scientific and Technical Research C...

70 PUBLICATIONS 741 CITATIONS

SEE PROFILE



Jorge Ruben Vega

National Scientific and Technical Research C...

87 PUBLICATIONS 517 CITATIONS

SEE PROFILE

Molecular Weight Control in a Starved Emulsion Polymerization of Styrene

Annia Salazar, Luis M. Gugliotta, Jorge R. Vega, and Gregorio R. Meira*

INTEC (Universidad Nacional del Litoral and CONICET), Güemes 3450, Santa Fe (3000), Argentina

A starved emulsion polymerization of styrene was investigated, with the aim of controlling the molecular weights of the produced polymer. The reactor was operated under a starved feed of a mixture of monomer and chain transfer agent (or “modifier”). *Tert*-dodecyl and *tert*-nonyl mercaptans were the employed modifiers. The starved operation produced a constant “most probable” molecular weight distribution along the polymerization. A mathematical model was developed to help interpret the effect of the modifier chain length. To adjust some of the model parameters, two batch experiments were carried out. In the starved polymerization with *tert*-dodecyl mercaptan, a mass transfer resistance to the modifier was required to fit the observed molecular weights. This extra mass transfer resistance could be neglected in the case of the (more water soluble) *tert*-nonyl mercaptan, however. The developed model also successfully predicts the batch experiments of Harelle et al. (*J. Appl. Polym. Sci.* **1994**, 52, 1105–1113).

Introduction

The molecular weight distribution (MWD) of a polymer produced in an emulsion polymerization is a basic characteristic that determines its processability and final use properties. For example, (i) the scrub resistance of a paint increases with the molecular weight; (ii) in a press adhesive, broad MWDs are required, with a high molecular weight fraction for providing mechanical resistance and a low molecular weight fraction for ensuring adhesion; and (iii) in a photocopier toner, narrow MWDs with low average molecular weights are specified.

The “compartmentalization” of free radicals in an emulsion polymerization determines that high molecular weights are obtained unless chain transfer agents (or “modifiers”) are incorporated in the reaction (Lichti et al., 1982; Gilbert, 1995).

Consider first the molecular weight control by chain transfer in a homogeneous free-radical polymerization. If most of the polymer is generated by chain transfer to the modifier, then the instantaneous MWD will exhibit a Schulz–Flory or “most probable” distribution, with the number-average molecular weight determined as follows:

$$\bar{M}_n = \left(\frac{k_p}{k_{tx}} \right) \frac{N_S}{N_X} = \left(\frac{1}{C_X} \right) \frac{N_S}{N_X} \quad (1)$$

where k_p is the propagation rate constant, k_{tx} is the transfer to the modifier rate constant, and N_S and N_X are the moles of monomer and modifier, respectively. From solution polymerization experiments, “true” C_X ratios ($= k_{tx}/k_p$) are obtained. A starved feed with a fixed monomer/modifier ratio along the polymerization allows us to maintain N_S/N_X constant, and therefore the accumulated MWD will also be Schulz–Flory. More generally, any arbitrary accumulated MWDs wider than Schulz–Flory could be in principle produced through an appropriate variation of N_S/N_X along the reaction.

For the solution polymerization of St with mercaptans containing from 9 to 13 carbon atoms, C_X values in the range 15–25 have been reported (Brandrup and Immergut, 1975).

In emulsion polymerizations, eq 1 is still valid but with the global ratio N_S/N_X replaced by $[S]_p/[X]_p$, where $[S]_p$ and $[X]_p$ respectively represent the concentrations of monomer and of modifier in the polymer particles. To calculate $[S]_p$ and $[X]_p$, the distribution of monomer and modifier between the phases must be known. If the two reagents are scarcely water-soluble and equally distributed in the organic phases, then $[S]_p/[X]_p \approx N_S/N_X$. In this case, eq 1 may be applied to find the monomer/modifier feed ratio that is required in a starved polymerization to produce a specified \bar{M}_n . For the monomer, the thermodynamic equilibrium assumption is normally verified. This is not the case of the long-chain modifiers, however; due to a restricted mass transfer to their flow from the monomer–modifier droplets into the polymer phase during intervals I and II (Nomura et al., 1994).

From the measurements of (a) the total number of moles of monomer and modifier N_S and N_X and/or (b) the accumulated \bar{M}_n values along a batch emulsion polymerization, different “effective” C_X ratios can be defined (Dietrich et al., 1988). Effective C_X values close to unity indicate that the monomer-to-modifier ratio remains constant along a batch polymerization; values lower than unity indicate that the average molecular weights decrease along the reaction; and values higher than unity indicate the opposite. In Table 1, typical effective C_X ratios for the batch emulsion polymerization of St with five scarcely water-soluble mercaptans are presented.

Effective ratios are about 1 order of magnitude below true C_X values. The reason for this is that the restricted modifier flow from the monomer–modifier phase into the polymer phase determines that the modifier concentration in the polymer particles is below equilibrium conditions. Also, effective C_X values are quite sensitive to the modifier chain length, due to the decreased water

* To whom correspondence should be addressed. Fax: 54-42-550944, E-mail: gmeira@polime1.arcrde.edu.ar.

Table 1. Emulsion Polymerization of St at 70 °C: Effective Ratio $C_X = k_{fx}/k_p$ for Five Different Mercaptans^a

X ₉	X ₁₀	X ₁₁	X ₁₂	X ₁₃	reference
	4.4 ^b , 5.2 ^c		1.5 ^b , 2.2 ^c		Dietrich et al. (1988)
2.00 ^c		1.00 ^c	0.51 ^c	0.29 ^c	Harelle et al. (1994)
1.95			0.31		this work

^a See symbols in the Nomenclature. ^b Adjusted from \bar{M}_n data obtained in batch experiments in conjunction with the mathematical model of Broadhead et al. (1985). ^c Calculated in batch experiments from global modifier to monomer ratios.

solubility (and diffusion rates) of the larger molecular-weight modifiers with respect to the smaller.

Several MWD control techniques for emulsion polymerizations have been developed; and in what follows such techniques are classified according to the employed reactor type.

Consider first the batch emulsion polymerizations. The early works by Bianchi et al. (1957), and Schulz and Romantowski (1965) investigated the effects of manipulating UV or γ radiation for controlling MWDs. Uraneck and Burleigh (1970) have tested a homologous series of commercial mercaptans for controlling the molecular weights of polystyrene (PS) and of styrene-butadiene copolymers. Weerts et al. (1991) have investigated the role of poorly water-soluble mercaptans in the homopolymerization of butadiene (B), observing that dodecyl mercaptans inhibit the formation of heavily cross-linked networks. Suddaby et al. (1996) and Bon et al. (1997) have respectively utilized "catalytic chain transfer agents" and the so-called "controlled radical polymerization technique" for producing materials of low molecular weight and polydispersity.

For an emulsion copolymerization of styrene (St) and B carried out in a continuous stirred-tank reactor (CSTR), Gugliotta et al. (1991) theoretically investigated the periodic forcing of the modifier feed, with the aim of broadening the MWD. Vega et al. (1995a,b) theoretically investigated the intermediate injection of a modifier in a continuous copolymerization of St and B carried out in a train of CSTRs, to (i) control the MWD obtained under steady-state conditions and (ii) reduce the off-spec product between steady states.

Several publications have appeared on the molecular weight control of semibatch emulsion polymerizations. Uraneck and Burleigh (1971) experimentally studied the addition of mercaptans along a St-B copolymerization, with the aim of reducing the final polydispersity. Baus (1985) investigated the addition of modifiers along the reaction, as a means of broadening the MWD of polyacrylic press adhesives.

Assuming a starved emulsion copolymerization of St and butyl acrylate, Paine et al. (1995) patented a

technique for controlling the MWD through a slow addition of modifier and preemulsified monomer; but no experimental validation of the method was presented. Harelle et al. (1994) carried out a slow semi-batch and preseeded polymerization for controlling the MWD of PS. However, starved conditions for the monomer and the modifier were not reached; and relatively broad MWDs were obtained.

Many of the mathematical models developed for emulsion polymerizations consider preseeded systems; and this approach has the advantage of avoiding the less known stage of the process, i.e., the particle nucleation period during interval I. For unseeded and starved emulsion polymerizations, no specific models have as yet been developed. In an ideal starved and unseeded system, the particle nucleation period is short with respect to the total reaction time; the monomer droplets volume is negligible along the polymerization; and an unrestricted and instantaneous mass transfer of the starved reagents into the polymer particles is verified. In a real situation, however, the particle nucleation can be affected by the starved feed rate; the existence of a separate monomer/modifier droplets phase is inevitable; and some of the reactions may be diffusion-controlled due to mass transfer restrictions between phases.

In this work, the starved and unseeded emulsion polymerization of St with *tert*-nonyl mercaptan (X₉) or *tert*-dodecyl mercaptan (X₁₂) is experimentally investigated, with the aim of producing a polymer of a constant MWD. Also, a simple mathematical model of the process is used, to help interpret the observed measurements.

Experimental Work

Two batch and three starved experiments were carried out at 70 °C in a 1 dm³ glass reactor. The reactor was equipped with a modified anchor stirrer, a sampling system, and a N₂ inlet. The temperature was controlled with a thermostatic bath and monitored with a digital thermometer. A stirring rate of 270 rpm was used. In the starved runs, a syringe pump allowed a continuous injection of the St-mercaptan mixtures.

The recipes are given in Table 2. They correspond closely to the recipes applied by Harelle et al. (1994), which are presented in Table 3. Our batch experiments B1 and B2 respectively involve the use of mercaptans X₁₂ and X₉, with an initial concentration of 1 ppm (parts per hundred monomer). In the starved experiments S1 and S2, X₁₂ at 1 and 0.5 ppm was used. In the starved experiment S3, X₉ at 1 ppm was employed.

Deionized water was used throughout the work. The emulsifier, the initiator, and the buffer salt were applied

Table 2. Applied Recipes

	batch expts		starved expts		
	B1 (g)	B2 (g)	S1 ^a (g)	S2 ^b (g)	S3 ^c (g)
monomer (St)	130.7	129.33	136.5	136.0	137.0
modifier (mercaptans)					
X ₉		1.315 ^d			1.384 ^e
X ₁₂	1.330 ^f		1.378 ^g	0.6954 ^h	
initiator (K ₂ S ₂ O ₈)	0.2335	0.2370	0.4000	0.4098	0.4074
emulsifier (SDS) ⁱ	2.620	2.6084	3.917	3.933	3.905
buffer (NaCO ₃ H)	0.1900	0.1952	0.2143	0.2744	0.1990
deionized water	515.6	516.2	540.7	516.9	515.5

^a 0.3283 g/min St-X₁₂ added along 420 min. ^b 0.3392 g/min St-X₁₂ added along 403 min. ^c 0.3376 g/min St-X₉ added along 410 min. ^d 0.008202 moles. ^e 0.008633 moles. ^f 0.006571 moles. ^g 0.006808 moles. ^h 0.003436 moles. ⁱ Sodium dodecyl sulfate.

Table 3. Batch Recipes of a Previous Publication^a

monomer (St)	100
modifier (mercaptans) ^b	
X ₉ (95% purity)	1.0
X ₁₁ (93% purity)	1.0
X ₁₂ (97% purity)	1.0
X ₁₃ (45% purity)	1.0
initiator (K ₂ S ₂ O ₈)	0.15
emulsifier (SDS)	2.0
buffer (NaCO ₃ H)	0.15
deionized water	397.7

^a Recipes by Harelle et al. (1994) in parts per hundred monomer.

^b Each recipe involved a different mercaptan, with all other reagents as shown.

as received. The monomer was prepared as follows. Commercial-grade St (PASA S.A., Argentina) was washed several times with a 15% KOH solution, then washed with water until neutral wash waters were obtained, and finally dried with CaCl₂. X₉ and X₁₂ modifiers from Fluka AG (95% purity) were employed as received.

In the batch runs, the emulsifier and the buffer salt were first dissolved in 500 g of water and loaded into the reactor. Then monomer and modifier were loaded, and the temperature was stabilized at 70 °C. To start the polymerization, the initiator was dissolved in the remaining water and added into the reactor. In the semibatch runs, the reactor was charged with the emulsifier–buffer solution, the temperature was stabilized at 70 °C, and the initiator solution was added. Immediately after, the St–mercaptan mixture was fed at approximately 0.33 g/min during around 400 min (see Table 2). The starved operations were adopted 5 times longer than the batch polymerizations for similar final monomer conversions.

Samples were withdrawn along the reactions and analyzed. The following was measured: (a) the total monomer conversion x , by gravimetry; (b) the unswollen number-average particle diameter $d_{p,unsw}$, with a Brookhaven BI-2030 dynamic light scattering photometer; and (c) the MWDs and averages, with a Waters ALC220 size-exclusion chromatograph. In the starved reactions, the fractional monomer conversion x_f (based on the monomer added up to each time) was also gravimetrically determined.

The batch experimental results are presented in Figure 1. As expected, conversion is little dependent on the mercaptan nature. For X₁₂, both the number- and the weight-average molecular weights monotonically decrease. In the case of X₉, the opposite was observed, and the MWDs exhibited a bimodality and a larger polydispersity. In both experiments, the evolution of the monomer-unswollen particle diameters, $d_{p,unsw}$, were practically coincident and with narrow distributions. Furthermore, and even though not presented here, a similar evolution of the particle sizes was observed when the recipe did not include a modifier. All of these observations indicate that X₁₂ cannot be contributing significantly toward the independent formation of (larger) polymer particles via an independent miniemulsion mechanism.

The starved polymerization results are presented in Figure 2. In Figure 2a, it is seen that truly starved conditions were not reached, especially at the beginning of the operation where $x_f \approx 78\%$. Despite this, nearly constant average molecular weights could still be obtained (Figure 2c,d). Also, the MWDs measured along a polymerization were all practically coincident (see chromatograms of experiment S1 in Figure 3). The total

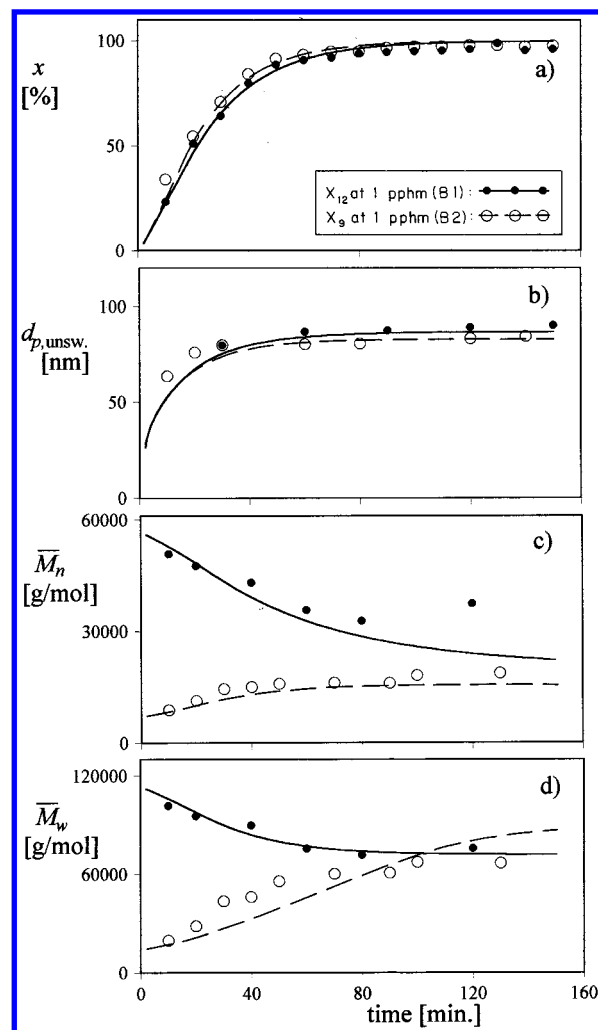


Figure 1. Batch experiments B1 and B2. Evolution of (a) total conversion (x), (b) unswollen particle diameter ($d_{p,unsw}$), (c) number-average molecular weight (\bar{M}_n), and (d) weight-average molecular weight (\bar{M}_w).

conversion is seen to increase in an approximately linear fashion (Figure 2b).

Mathematical Model and Simulation Results

A simple mathematical model for the emulsion polymerization of St was developed (see the Appendixes). It considers reactions in the aqueous and in the polymer phases (eqs A1–A8). All symbols are indicated in the Nomenclature.

The model is basically a simplification of that presented in Gugliotta et al. (1995a) for an emulsion polymerization of St and B. In that publication, the following was assumed: (a) a perfectly stirred reaction; (b) micellar nucleation according to the classical mechanism by Harkins (1947); (c) the gel effect, through a reduction of the termination rate with the volume fraction of polymer in the polymer phase, ϕ_p , according to the free volume approach presented in Broadhead et al. (1985); and (d) the MWD is mainly determined by chain transfer to the modifier and is unaffected by the termination reactions. In this work, the following further assumptions are adopted: (e) absence of impurities; (f) a monodisperse particle size distribution; (g) partition of the monomer between phases according to equilibrium, with constant partition coefficients; (h) a mass transfer resistance to the modifier flow across the

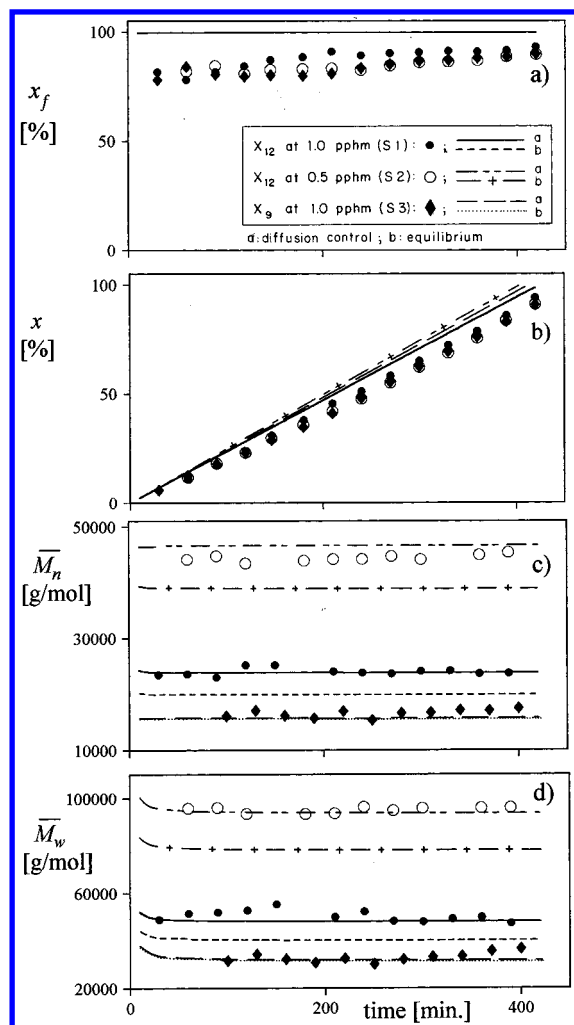


Figure 2. Starved experiments S1–S3 for molecular weight control. Evolution of (a) fractional conversion (x_f), (b) total conversion (x), (c) number-average molecular weight (\bar{M}_n), and (d) weight-average molecular weight (\bar{M}_w).

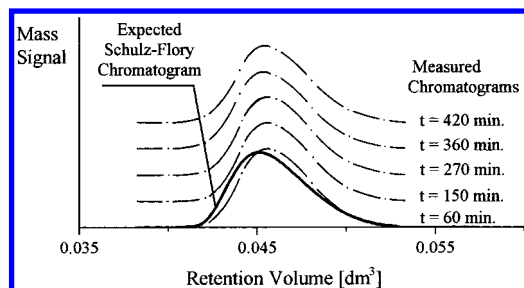


Figure 3. Chromatograms of experiment S1 (dashed traces) and simulated chromatogram of an equivalent Schulz–Flory distribution (continuous trace).

water film that recovers the monomer droplets (see Figure 4); (i) desorption of primary modifier radicals; and (j) the monomer droplets are not stabilized by the scarcely water soluble modifiers.

When a starved process is simulated with the above assumptions, it results that the nucleation stage is completed during a short period at the beginning of the reaction. This is so because the employed nucleation model only requires the presence of emulsifier and initiator to generate the particles and is quite independent of the monomer concentration.

The mathematical model is represented by eqs A9–A38. It cannot be solved as it is, because it does not

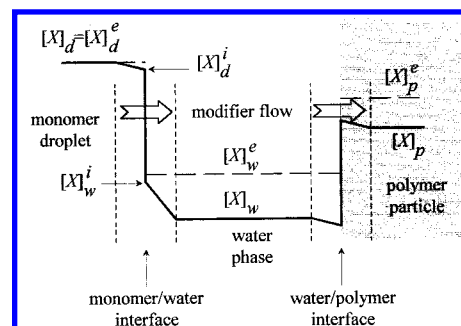


Figure 4. Concentration profile of the modifier along the three phases during intervals I and II (schematic). The dashed vertical lines indicate the films limits where mass transfer restrictions are concentrated. The arrows indicate the flow of modifier.

include an expression for the variation of the total surface area of monomer droplets, A_d ; that appears in eq A24. To circumvent this problem, the two extra assumptions that follow are adopted.

(1) In the batch experiments, the modifier is considered in equilibrium between the phases; and an effective C_X ratio is adjusted. (This is equivalent to neglecting the second term in the denominator of eq A24.)

(2) In the starved experiments, the C_X values adjusted in (1) is applied, and the product $k_{X,wt} A_d$ in eq A24 is treated as a single adjustment parameter.

The model parameters are presented in Table 4 and in the last row of Table 1. Most of the parameters were directly taken from the literature. Except for the product $k_{X,wt} A_d$, the less known and/or highly sensitive parameters were adjusted within reported literature values, using the batch experimental results. The applied procedure was as follows. From the batch polymerization measurements, the total conversion, x , the average particle diameter, $d_{p,unsw}$, and the average molecular weights were fit via a simultaneous adjustment of the following parameters, starting from known literature values: the emulsifier surface coverage capacity, A_s ; the rate constant of radical absorption into the particles, k_a ; the propagation rate constant in the polymer phase, k_p ; the overall mass transfer resistance of the modifier radicals represented by $D_{wX} \delta$ in eq A33; and an effective k_{fX} (or C_X). Finally, the product $k_{X,wt} A_d$ was adjusted from the measurements of \bar{M}_n along the starved reactions.

Through the mentioned adjustment procedure, a global mathematical model was obtained; and some of the adjusted parameters resulted slightly different from the best-known values of such parameters. For example, the adopted value of k_p is about 30% below the value reported in Gilbert (1995); that was obtained through an elaborate laser-pulsed technique. The parameter biases allow us to compensate for the measurements errors and for all other unknown phenomena not accounted for in our model (e.g., the presence of impurities).

Batch Experiments. For the batch experiments, Figure 1 shows that all measured variables are reasonably well predicted by the model. Even though not shown, the monomer–modifier droplets disappear at $t \approx 25$ min for both mercaptans. The differences in conversion are due to the larger radical desorption coefficient k_{de} for X_9 when compared with that of X_{12} (eq A33). The average molecular weight profiles are as expected, according to the adjusted C_X ratios. In Table 1 it is seen that the applied adjustment procedure yielded C_X ratios that are similar to those reported by

Table 4. Model Parameters at 70 °C

A_S		$3.00 \times 10^7 \text{ dm}^2 \text{ mol}^{-1}$
$D_{wX} \delta$	(X = X ₉)	$0.40 \times 10^{-7} \text{ dm}^2 \text{ min}^{-1}$
	(X = X ₁₂)	$9.10 \times 10^{-7} \text{ dm}^2 \text{ min}^{-1}$
$[E]_{\text{CMC}}$		$9.00 \times 10^{-3} \text{ mol dm}^{-3}$
f		0.6
k_a		$1.00 \times 10^{-3} \text{ dm min}^{-1}$
k_d		$1.30 \times 10^{-3} \text{ min}^{-1}$
k_{fs}		$1.17 \text{ dm}^3 \text{ mol}^{-1} \text{ min}^{-1}$
k_{fx}	(X = X ₉)	$3.64 \times 10^4 \text{ dm}^3 \text{ mol}^{-1} \text{ min}^{-1} \text{ }^a$
	(X = X ₁₂)	$5.85 \times 10^3 \text{ dm}^3 \text{ mol}^{-1} \text{ min}^{-1} \text{ }^a$
k_p		$1.88 \times 10^4 \text{ dm}^3 \text{ mol}^{-1} \text{ min}^{-1}$
k_{tp}		$1.30 \times 10^7 \text{ dm}^3 \text{ mol}^{-1} \text{ min}^{-1}$
		$2.90 \times 10^7 \text{ dm}^3 \text{ mol}^{-1} \text{ min}^{-1} \text{ }^b$
k_{tw}		$8.40 \times 10^9 \text{ dm}^3 \text{ mol}^{-1} \text{ min}^{-1}$
$k_{X,wt} A_d$	(X = X ₉ , X ₁₂)	$5.00 \times 10^4 \text{ dm}^3 \text{ min}^{-1}$
K_{sdw}		1.81×10^3
K_{swp}		9.26×10^{-4}
K_{Xdw}	(X = X ₉)	7.00×10^5
	(X = X ₁₂)	4.90×10^7
K_{Xwp}	(X = X ₉)	2.22×10^{-6}
	(X = X ₁₂)	3.14×10^{-8}
ρ_p		$1.04 \times 10^3 \text{ g dm}^{-3}$
$D_{wX} \delta$	(X = X ₁₁)	$2.37 \times 10^{-7} \text{ dm}^2 \text{ min}^{-1}$
	(X = X ₁₃)	$9.50 \times 10^{-7} \text{ dm}^2 \text{ min}^{-1}$
k_{fx}	(X = X ₁₁)	$2.21 \times 10^4 \text{ dm}^3 \text{ mol}^{-1} \text{ min}^{-1} \text{ }^a$
	(X = X ₁₃)	$5.76 \times 10^3 \text{ dm}^3 \text{ mol}^{-1} \text{ min}^{-1} \text{ }^a$
K_{Xdw}	(X = X ₁₁)	2.50×10^6
	(X = X ₁₃)	4.90×10^7
K_{Xwp}	(X = X ₁₁)	6.15×10^{-7}
	(X = X ₁₃)	3.14×10^{-8}

^a "Effective" rate. ^b Resulting range for all experiments, as predicted by the free-volume theory.

Harelle et al. (1994). This is consistent with our model predictions, which indicate that the global modifier-to-monomer ratio is always close to that same value but in the polymer particles (with a maximum difference of around 7% at the beginning of the polymerization).

To further validate the developed model, the batch experiments by Harelle et al. (1994) involving four tertiary mercaptans were simulated (Table 3 and Figure 5). For X₉ and X₁₂, the parameters presented in the upper part of Table 4 were directly applied. For X₁₁ and X₁₃, the parameters shown in the lower part of Table 4 were used. In all simulations, equilibrium conditions for the mercaptans were assumed. Figure 5 shows that reasonably good predictions were obtained.

Starved Experiments. Consider the starved polymerization results of Figures 2, 3, and 6. The following may be noted.

The predicted fractional monomer conversions are all close to 100%, while the corresponding measurements are below that value. Also, the model predictions for the total monomer conversions are above the experimental points. The deviations are possibly due to the relatively crude nucleation model employed (Figure 2a,b).

In a transfer-dominated free-radical polymerization, the instantaneously produced polymer presents a Schulz–Flory MWD (eq A38). Therefore, under perfect molecular weight control, the final accumulated MWD will be also Schulz–Flory. To verify this, in Figure 3 the chromatograms of run S1 are compared with a simulated chromatogram representing a Schulz–Flory distribution that was calculated from the predicted value of \bar{M}_n .

For comparison reasons, starved experiments were also simulated assuming equilibrium conditions for the modifiers; and the predictions are represented in Figure 2. For X₁₂, the calculated molecular weights assuming

adjusted in this work, based on Brandrup and Immergut (1975)
adjusted in this work, based on Nomura et al. (1982)
adjusted in this work, based on Nomura et al. (1982)
Harelle et al. (1994)
López de Arbina et al. (1996)
adjusted in this work
López de Arbina et al. (1996)
López de Arbina et al. (1996)
adjusted in this work
adjusted in this work
adjusted in this work, based on Gilbert (1995),
Broadhead et al. (1985), and Lopez de Arbina et al. (1996)
Broadhead et al. (1985)

López de Arbina et al. (1996)
adjusted in this work
Gugliotta et al. (1995b)
Gugliotta et al. (1995b)
Nomura et al. (1994)
Nomura et al. (1994)
Nomura et al. (1994)
Nomura et al. (1994)
Brandrup and Immergut (1975)
adjusted in this work, based on Nomura et al. (1982)
adjusted in this work, based on Nomura et al. (1982)
Harelle et al. (1994)
Harelle et al. (1994)
Nomura et al. (1994)
Nomura et al. (1994)
Nomura et al. (1994)
Nomura et al. (1994)
Nomura et al. (1994)

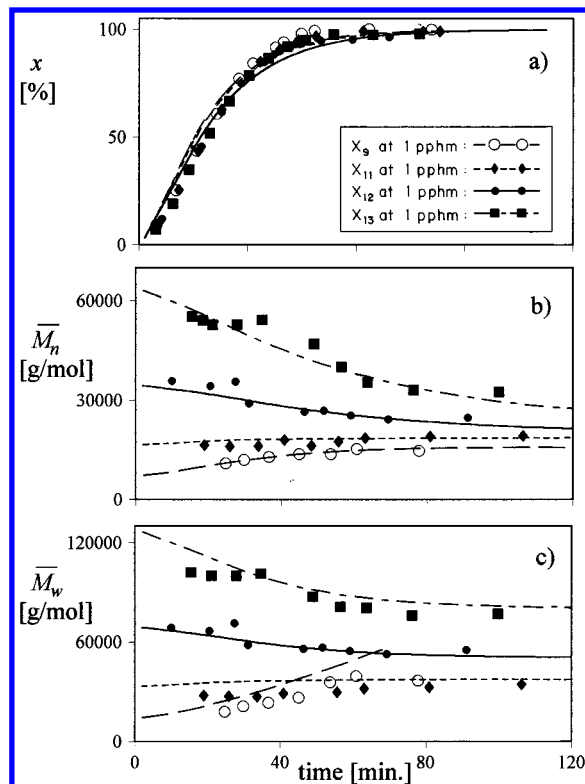


Figure 5. Batch experimental results by Harelle et al. (1994) (symbols) and corresponding predictions of our model (traces). Evolution of (a) total conversion (x), (b) number-average molecular weight (\bar{M}_n), and (c) weight-average molecular weight (\bar{M}_w).

equilibrium are lower than the molecular weights estimated considering a mass transfer resistance. In the case of X₉, its higher water-solubility produces a negligible mass-transfer resistance; and consequently both estimated molecular weights coincide.

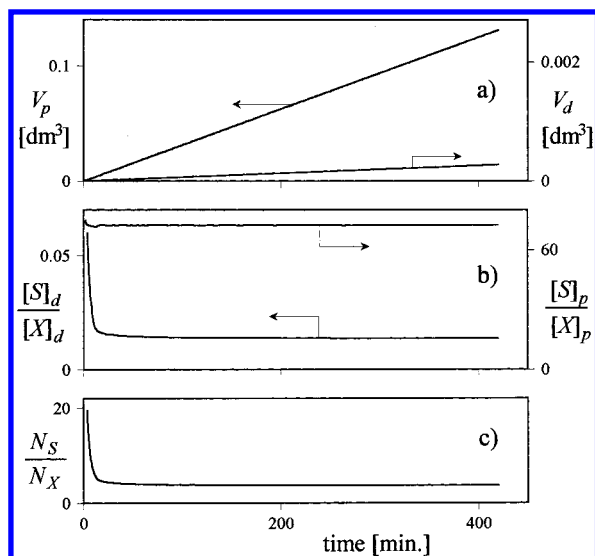


Figure 6. Starved experiment S1. Theoretical estimation of (a) particles and droplets phase volumes (V_p , V_d), (b) concentration ratio between monomer and modifier in the polymer and in the droplets phases $[S]_p/[X]_p$ and $[S]_d/[X]_d$, respectively, and (c) global moles ratio N_S/N_X .

For experiment S1 with X_{12} , Figure 6 shows the predicted evolutions of (i) the volumes of polymer and droplets phases V_p and V_d , (ii) the ratio of concentrations of monomer and modifier in the polymer phase $[S]_p/[X]_p$ and in the droplets phase $[S]_d/[X]_d$, and (iii) the global molar ratio N_S/N_X . Even though not shown, the estimated fractional conversion of X_{12} was practically constant and below 100% ($\approx 83\%$), as a result of the mass transfer restriction. Both V_p and V_d grow in an approximately linear fashion; and as expected, even at the final time V_d is relatively small. For X_{12} , $[S]_p/[X]_p$ is several times larger than $[S]_d/[X]_d$ as a consequence of the restricted mass transfer; with the effect that X_{12} accumulates outside the reaction site. The essentially constant values of $[S]_p/[X]_p$ explain the observed constant MWDs.

For experiment S3 with X_9 , the simulation results indicate that $[S]_p/[X]_p \approx [S]_d/[X]_d \approx N_S/N_X$; with the modifier fractional conversion the value is always close to 100%. Thus, eq 1 can be applied to calculate the monomer to modifier feed ratio that is required to produce a specified \bar{M}_n through a starved operation. For X_{12} , no simple way of calculating the starved feed ratio for a specified \bar{M}_n is available. Instead, numerical simulations via a detailed polymerization model such as the one here presented must be applied.

Concluding Remarks

The quasi-starved feed of a monomer–modifier mixture along an unseeded emulsion polymerization of St allows production of a polymer with a constant Schulz–Flory (or “most probable”) MWD.

The developed mathematical model has proven adequate for predicting the batch experiments but presents some limitations in the case of the starved and unseeded operations. This was to be expected, considering the crude nucleation model employed and the fact that most adjustable parameters were modified to reproduce the batch measurements. Most emulsion polymerization models adopt effective C_X ratios and

assume an instantaneous equilibrium between phases for the modifier. However, the highly reduced monomer droplets area in the starved operation with respect to the batch process determines that a mass transfer resistance must be introduced for the highly water-insoluble modifiers. As a consequence of this resistance, in the case of X_{12} the monomer–modifier ratio is several times lower in the droplets than in the polymer particles.

In the batch experiments, the slower-reacting X_{12} mercaptan seems preferable to X_9 , because in the former case narrower and unimodal MWDs were obtained. However, for molecular weight control through starved operations, X_9 is preferable, because its lower mass transfer resistance and higher reactivity ensures starved conditions in a shorter reaction time. Furthermore, in the case of X_9 , eq 1 may be simply extended to determine the monomer to modifier feed ratio that is required to produce a specified \bar{M}_n .

Acknowledgment

We thank CONICET and Universidad Nacional del Litoral for the financial support, M. C. Brandolini and J. L. Castañeda (INTEC) for their help with the experimental work, and PASA S.A. for providing us with some of the reagents.

Nomenclature

Reagents and Products

E = emulsifier

I = initiator

P_n = polystyrene produced in the polymer phase

$P_{n,w}$ = polystyrene oligomer produced in the aqueous phase

R_c^* = primary initiator radical produced by thermal decomposition in the aqueous phase

St = styrene monomer

S_n^* = propagating radical of chain length n , in the polymer phase

$S_{n,w}^*$ = propagating radical of chain length n , in the aqueous phase

X = chain transfer agent or modifier

X_9 = *tert*-nonyl mercaptan

X_{10} = *n*-decyl mercaptan

X_{11} = *tert*-undecyl mercaptan

X_{12} = *tert*-dodecyl mercaptan

X_{13} = *tert*-tridecyl mercaptan

X^* = modifier radical

Main Variables

A_p = total surface area of the polymer particles (dm^2)

A_m = total surface area of the emulsifier micelles (dm^2)

d_p = monomer-swollen number-average particle diameter (dm)

$d_{p,unsw}$ = unswollen number-average particle diameter (nm)

$F_{j,in}$ = inlet molar flow rate of reagent j (mol/min)

$[j]$ = concentration of reagent j (mol/ dm^3)

m = defined by eq A30 (dimensionless)

M = molecular weight (g/mol)

\bar{M}_n, \bar{M}_w = number- and weight-average molecular weight (g/mol)
 n = chain length (dimensionless)
 \bar{n} = average number of radicals per particle (dimensionless)
 N_j = moles of reagent j
 $N_{S,b}$ = moles of bound (or polymerized) St
 N_S^0 = moles of initially loaded St
 N_p = total number of polymer particles in the reactor (dimensionless)
 $Q_i = \sum_n n^i [P_n] = i$ th moment ($i = 0, 1, 2$) of the number chain-length distribution $[P_n](n)$ (mol/dm³)
 R_i = initiation rate (mol/min)
 t = time (min)
 t_f = final reaction time (min)
 V_d = monomer-modifier droplets phase volume (dm³)
 V_{H_2O} = pure water volume (dm³)
 v_p = swollen number-average volume of a latex particle (dm³)
 V_p = polymer phase volume (dm³)
 V_w = aqueous phase volume (dm³)
 $w(M)$ = weight MWD (mass vs g/mol)
 x = total conversion (dimensionless)
 x_f = fractional conversion (dimensionless)
 Y = defined by eq A31 (dimensionless)

Model Parameters

A_d = total surface area of the monomer-modifier droplets (dm²)
 A_S = emulsifier surface coverage capacity (dm²)
 $C_X = k_{IX}/k_p$ effective ratio (dimensionless)
 D_{wX} = diffusion coefficient of X^\bullet in the water phase (dm²/min)
 $[E]_{CMC}$ = emulsifier critical micellar concentration (mol/dm³)
 f = initiator efficiency (dimensionless)
 k_a = rate constant of radical absorption into the polymer particles (dm/min)
 k_d = rate constant of initiator decomposition (min⁻¹)
 k_{de} = rate constant of radical desorption from the polymer particles (min⁻¹)
 k_{IS} = rate constant of transfer to the monomer (dm³ mol⁻¹ min⁻¹)
 k_{IX} = rate constant of transfer to the modifier (dm³ mol⁻¹ min⁻¹)
 k_p = propagation rate constant in polymer phase (dm³ mol⁻¹ min⁻¹)
 $k_{p,w}$ = propagation rate constant in water phase (dm³ mol⁻¹ min⁻¹)
 k_{pc} = rate constant for generation of primary monomeric free radicals (dm³ mol⁻¹ min⁻¹)
 k_{tp} = rate constant of radical termination in polymer phase (dm³ mol⁻¹ min⁻¹)
 k_{tw} = rate constant of radical termination in water phase (dm³ mol⁻¹ min⁻¹)
 $k_{X,wt}$ = modifier mass-transfer coefficient (dm/min)
 $K_{jd,w}, K_{jwp}$ = partition coefficients of reagent j (St or X) between the monomer droplets and the aqueous phase, and between the aqueous and the polymer phases, respectively (dimensionless)
 M_S = St molecular weight (g/mol)
 M_X = modifier molecular weight (g/mol)
 N_A = Avogadro's constant (mol⁻¹)

Greek Symbols

α, α' = variables defined by eqs A28 and A29, respectively (dimensionless)
 δ = ratio of water-side resistance to overall mass-transfer resistance for X^\bullet ($0 < \delta \leq 1$) (dimensionless)
 ρ_p = polymer density (g/dm³)
 ρ_S = St density (g/dm³)
 ρ_X = modifier density (g/dm³)
 ϕ_p = polymer volume fraction in polymer phase (dimensionless)

Subscripts

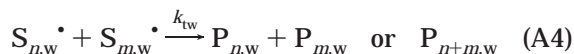
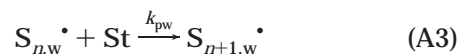
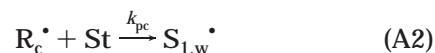
d = monomer droplets phase
 n = chain length (dimensionless)
 p = polymer phase
 w = aqueous phase

Superscripts

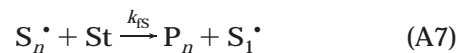
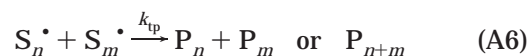
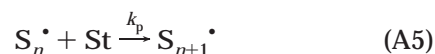
e = equilibrium conditions
 i = interface

Appendix A: Proposed Kinetics and Mathematical Model

Kinetic Scheme. In the aqueous phase, the following mechanism is assumed:



In the polymer phase, the mechanism is as follows:



The termination reactions of eqs A4 and A6 are only considered for their contribution toward conversion but are neglected in the MWD calculation (Gugliotta et al., 1995a). Similarly, the monomer consumed in eq A3 is neglected for the calculation of the total conversion.

Differential Equations. From eqs A1 and A5–A8, the following balances may be respectively written for the moles of St, the moles of initiator, the moles of modifier, the total number of polymer particles, and the

first three moments of the number chain length distribution (see Gugliotta et al., 1995a):

$$\frac{dN_S}{dt} = F_{S,in} - k_p[S]_p^e \frac{\bar{n}N_p}{N_A} \quad (A9)$$

$$\frac{dN_I}{dt} = -k_d N_I \quad (A10)$$

$$\frac{dN_X}{dt} = F_{X,in} - k_{IX}[X]_p \frac{\bar{n}N_p}{N_A} \quad (A11)$$

$$\frac{dN_p}{dt} = \frac{A_m}{A_m + A_p} \left\{ R_I + k_{de} \frac{\bar{n}N_p}{N_A V_w} - k_{tw}[R^*]_w^2 \right\} V_w N_A \quad (A12)$$

$$\frac{d(V_p Q_0)}{dt} = (k_{IS}[S]_p^e + k_{IX}[X]_p) \frac{\bar{n}N_p}{N_A} \quad (A13)$$

$$\frac{d(V_p Q_1)}{dt} = \frac{dN_{S,b}}{dt} = k_p[S]_p^e \frac{\bar{n}N_p}{N_A} \quad (A14)$$

$$\frac{d(V_p Q_2)}{dt} = 2k_p[S]_p^e \frac{\bar{n}N_p}{N_A} \left(\frac{k_p[S]_p^e + k_{IX}[X]_p}{k_{IS}[S]_p^e + k_{IX}[X]_p} \right) \quad (A15)$$

Algebraic Equations. Assuming a monodisperse particle size distribution, the total areas of the polymer particles and of the emulsifier micelles during interval I are respectively calculated through

$$A_p = (6\pi^{1/2} V_p)^{2/3} N_p^{1/3} \quad (A16)$$

$$A_m = A_S(N_E - [E]_{CMC} V_w) - A_p \quad (A17)$$

The global volumes of monomer-modifier droplets, polymer particles, and aqueous phase are obtained from

$$V_d = \frac{M_S}{\rho_S} (N_S - [S]_p^e V_p - [S]_w^e V_w) + \frac{M_X}{\rho_X} (N_X - [X]_p V_p - [X]_w V_w) \quad (A18)$$

$$V_w = \frac{V_{H_2O}}{1 - \frac{M_S}{\rho_S} [S]_w^e} \quad (A19)$$

$$V_p = \frac{M_S N_{S,b}}{\rho_p \phi_p} \quad (A20)$$

The polymer volume fraction in the polymer phase is calculated as follows:

$$\phi_p = 1 - \frac{M_S}{\rho_S} [S]_p^e \quad (A21)$$

For the monomer, a distribution between phases according to equilibrium is assumed. Thus, the St molar concentrations in the polymer and the aqueous phases are given by

$$[S]_p^e = \frac{N_S}{K_{Sdw} K_{Swp} V_d + K_{Swp} V_w + V_p} \quad (A22)$$

$$[S]_w^e = \frac{N_S}{K_{Sdw} V_d + V_w + V_p/K_{Swp}} \quad (A23)$$

The modifier concentration in the polymer phase is obtained from the following expression (see derivation in Appendix B):

$$[X]_p = \frac{[X]_p^e}{1 + \frac{k_{IX} \bar{n} N_p / N_A}{k_{X,wt} A_d K_{Xwp}}} \quad \text{with } k_{IX} = C_X k_p \quad (A24)$$

where the modifier concentration under equilibrium conditions $[X]_p^e$ is obtained from:

$$[X]_p^e = \frac{N_X}{K_{Xdw} K_{Xwp} V_d + K_{Xwp} V_w + V_p} \quad (A25)$$

Equation A24 determines that for a high value of the monomer droplets area A_d and/or for a high partition coefficient K_{Xwp} (i.e., for mercaptans with high water solubility), then $[X]_p \approx [X]_p^e$. For example, K_{Xwp} for X_9 is 2 orders of magnitude larger than K_{Xwp} for X_{12} , and then $[X]_p \approx [X]_p^e$ for X_9 , while $[X]_p < [X]_p^e$ for X_{12} . High A_d values are observed in batch polymerizations during intervals I and II. However, under starved conditions, A_d can be several orders of magnitude smaller than in batch polymerizations and approximately constant along the reaction.

In aqueous phase, the following radical balance may be written:

$$R_I + k_{de} \frac{\bar{n}N_p}{N_A V_w} = k_a \frac{A_p}{V_T} [R^*]_w + k_{tw} [R^*]_w^2 \quad (A26)$$

with the initiation rate R_I given by

$$R_I = 2fk_d \frac{N_I}{V_w} \quad (A27)$$

The average number of radicals per particle is calculated from the following expression (Ugestald and Hansen, 1976):

$$\bar{n} = 0.5 \frac{2\alpha}{m + \frac{2\alpha}{m + 1 + \frac{2\alpha}{m + 2 + \dots}}} \quad (A28)$$

with

$$\alpha = \alpha' + m\bar{n} - \alpha^2 Y \quad (\text{A29})$$

$$\alpha' = \frac{R_I V_w V_p N_A^2}{N_p^2 k_{tp}} \quad (\text{A30})$$

$$m = \frac{k_{de} V_p N_A}{k_{tp} N_p} \quad (\text{A31})$$

$$Y = \frac{k_{tp} k_{tw} N_p^2}{\left(\frac{k_a A_p}{V_T}\right)^2 V_p V_w N_A^2} \quad (\text{A32})$$

In eq A31, the desorption rate coefficient k_{de} is calculated as in Nomura et al. (1982):

$$k_{de} = \frac{12 D_{wX} \delta k_{IX} [X]_p K_{Xwp}}{d_p^2 k_p [S]_p^e} \quad (\text{A33})$$

The total conversion x , the fractional conversion, x_f , and the number- and weight-average molecular weights can be computed as follows:

$$x = \frac{N_{S,b}}{N_S^0 + \int_0^t F_{S,in}(t) dt} \quad (\text{A34})$$

$$x_f = \frac{N_{S,b}}{N_{S,b} + N_S} \quad (\text{A35})$$

$$\bar{M}_n = M_S \frac{Q_1}{Q_0} \quad (\text{A36})$$

$$\bar{M}_w = M_S \frac{Q_2}{Q_1} \quad (\text{A37})$$

Finally, for a reaction mechanism where most of the polymer is produced by chain transfer to the modifier, it is well-known that the weight MWD of the instantaneously produced polymer, $w(M)$, responds to a Schulz-Flory distribution of the form

$$w(M) = \left(\frac{M}{\bar{M}_n}\right) \exp\left(-\frac{M}{\bar{M}_n}\right) \quad (\text{A38})$$

The instantaneous polydispersity is $\bar{M}_w/\bar{M}_n = Q_0 Q_2 / Q_1^2 \cong 2$.

Appendix B: Modifier Concentration in the Polymer Particles: Derivation of Equation A24

In Figure 4, a schematic concentration profile of the modifier along the three phases during intervals I and II is shown. The modifier is consumed only in the polymer phase, and therefore a permanent flow of this reagent from the monomer droplets and into the polymer particles is produced. Under equilibrium conditions, an unrestricted and instantaneous modifier transfer is established; which determines a maximum concentration of modifier in the polymer particles (dashed trace in Figure 4).

Nomura et al. (1994) showed that the modifier concentration in the polymer particles may be below

thermodynamic equilibrium; mainly as a consequence of a restricted mass transfer across the water film that covers the monomer droplets (continuous trace in Figure 4).

Under equilibrium conditions, the modifier splits between the three phases according to

$$K_{Xdw} = \frac{[X]_d^e}{[X]_w^e} \quad (\text{B1a})$$

$$K_{Xdw} K_{Xwp} = \frac{[X]_d^e}{[X]_p^e} \quad (\text{B1b})$$

Under steady-state conditions, the flow across the monomer-water interface must be equal to the consumption in the polymer particles, and therefore

$$k_{X,wt} A_d ([X]_w^i - [X]_w) = k_{IX} \frac{\bar{n} N_p}{N_A} [X]_p \quad (\text{B2})$$

Assuming an equilibrium partition at the interfaces, then we can write

$$K_{Xdw} = \frac{[X]_d^i}{[X]_w^i} \cong \frac{[X]_d}{[X]_w^i} \quad (\text{B3})$$

and

$$K_{Xwp} \cong \frac{[X]_w}{[X]_p} \quad (\text{B4})$$

Finally, since $[X]_d^e \cong [X]_d$, the modifier concentration in the polymer phase may be found by replacing eqs B1, B3, and B4 into eq B2, yielding

$$[X]_p = \frac{[X]_p^e}{1 + \frac{k_{IX} \bar{n} N_p / N_A}{K_{X,wt} A_d K_{Xwp}}} \quad \text{with } k_{IX} = C_X k_p \quad (\text{B5})$$

Equation B5 is only applicable while a separate monomer phase is present. Note that the second term in the denominator of eq B5 is positive, and therefore $[X]_p \leq [X]_p^e$.

Literature Cited

- Baus, R. E., U.S. Patent 4,501,845, 1985.
- Bianchi, J. P.; Price, F. P.; Zimen, B. H. "Monodisperse" Polystyrene. *J. Polym. Sci.* **1957**, *25*, 27.
- Bon, S. A. F.; Bosveld, M.; Klumperman, B.; German, A. L. Controlled Radical Polymerization in Emulsion. *Macromolecules* **1997**, *30*, 324-326.
- Brandrup, J.; Immergut, E. H. *Polymer Handbook*, Second Edition, Wiley-Interscience, J. Wiley & Sons: New York, 1975.
- Broadhead, T. O.; Hamielec, A. E.; MacGregor, J. F. Dynamic Modeling of the Batch, Semi-Batch and Continuous Production of Styrene/Butadiene by Emulsion Polymerization. *Makromol. Chem., Suppl.* **1985**, *10/11*, 105-128.
- Dietrich, B. K.; Pryor, W. A.; Wu, S. J. Chain Transfer Constants of Mercaptans in the Emulsion Polymerization of Styrene. *J. Appl. Polym. Sci.* **1988**, *36*, 1129-1141.
- Gilbert, R. G. *Emulsion Polymerization. A Mechanistic Approach*; Academic Press: London, 1995.
- Gugliotta, L. M.; Couso, D. A.; Meira, G. R. MWD Control in Continuous Free-Radical Polymerizations through Forced Oscillations of the Transfer Agent Feed. *J. Appl. Polym. Sci.* **1991**, *42*, 2903-2913.

- Gugliotta, L. M.; Brandolini, M. C.; Vega, J. R.; Iturralde, E. O.; Azum, J. L.; Meira, G. R. Dynamic Model of a Continuous Emulsion Copolymerization of Styrene and Butadiene. *Polym. React. Eng.* **1995a**, 3 (3), 201–233.
- Gugliotta, L. M.; Arotçarena, M.; Leiza, J. R.; Asua, J. M. Estimation of Conversion and Copolymer Composition in Semi-continuous Emulsion Polymerization using Calorimetric Data. *Polymer* **1995b**, 36 (10), 2019–2023.
- Harelle, L.; Pith, T.; Hu, G.; Lambla, M. Chain Transfer Behavior of Fractionated Commercial Mercaptans in Emulsion Polymerization of Styrene. *J. Appl. Polym. Sci.* **1994**, 52, 1105–1113.
- Harkins, W. D. A General Theory of the Mechanism of Emulsion Polymerization. *J. Am. Chem. Soc.* **1947**, 69, 1428–1444.
- Lichti, G.; Gilbert, R. G.; Napper, D. H. Theoretical Predictions of the Particle Size and Molecular Weight Distributions in Emulsion Polymerizations. In *Emulsion Polymerization*; Piirma, I., Ed.; Academic Press: New York, 1982; pp 93–144.
- López de Arbina, L.; Barandiaran, M. J.; Gugliotta, L. M.; Asua, J. M. Emulsion Polymerization: Particle Growth Kinetics. *Polymer* **1996**, 37 (26), 5907–5916.
- Nomura, M.; Minamino, Y.; Fujita, K.; Harada, M. The Role of Chain Transfer Agents in the Emulsion Polymerization of Styrene. *J. Polym. Sci., Polym. Chem. Ed.* **1982**, 20, 1261–1270.
- Nomura, M.; Suzuki, H.; Tokunaga, H.; Fujita, K. Mass Transfer Effects in Emulsion Polymerization Systems. I. Diffusional Behavior of Chain Transfer Agents in the Emulsion Polymerization of Styrene. *J. Appl. Polym. Sci.* **1994**, 51, 21–31.
- Paine, A. J.; Pontes, F. M.; Moffat, K. A. U.S. Patent 5,444,140, 1995.
- Schulz, G. V.; Romantowski, J. Emulsionspolymerisation von Styrol. *Makromol. Chem.* **1965**, 85, 195.
- Suddaby, K. G.; Haddleton, D. M.; Hastings, J. J.; Richards, S. N.; O'Donnell, J. P. Catalytic Chain Transfer for Molecular Weight Control in the Emulsion Polymerization of Methyl Methacrylate and Methyl Methacrylate–Styrene. *Macromolecules* **1996**, 29, 8083–8091.
- Ugelstad, J.; Hansen, F. K. Kinetics and Mechanism of Emulsion Polymerization. *Rubber Chem. Technol.* **1976**, 49, 536–609.
- Uraneck, C. A.; Burleigh, J. E. Molecular Weight Distribution of Polystyrene and of Butadiene–Styrene Copolymers Prepared in Emulsion Systems. *J. Appl. Polym. Sci.* **1970**, 14 (2), 267–284.
- Uraneck, C. A.; Burleigh, J. E. Modification of Emulsion Polymerization by Multiple Addition of Modifier. *J. Appl. Polym. Sci.* **1971**, 15 (7), 1757–1768.
- Vega, J. R.; Gugliotta, L. M.; Brandolini, M. C.; Meira, G. R. Steady-State Optimization in a Continuous Emulsion Copolymerization of Styrene and Butadiene. *Lat. Am. Appl. Res.* **1995a**, 25, 207–214.
- Vega, J. R.; Gugliotta, L. M.; Meira, G. R. Continuous Emulsion Copolymerization of Styrene and Butadiene. Reduction of the Off-Spec Product between Steady-States. *Lat. Am. Appl. Res.* **1995b**, 25, 77–82.
- Weerts, P. A.; van der Loos, J. L. M.; German, A. L. Emulsion Polymerization of Butadiene, 4. *Makromol. Chem.* **1991**, 192, 2009–2019.

Received for review January 5, 1998

Revised manuscript received June 8, 1998

Accepted June 10, 1998

IE980009Y